

# A model of fluid flow in a scraped-surface heat exchanger

by **B. R. Duffy, S. K. Wilson,<sup>1</sup>**

Department of Mathematics, University of Strathclyde,  
Livingstone Tower, 26 Richmond Street, Glasgow G1 1XH

**M. E. M. Lee**

Faculty of Mathematical Studies, University of Southampton,  
Highfield, Southampton SO17 1BJ

and **N. H. Taylor**

Chemtech International Ltd, 448 Basingstoke Road, Reading RG2 0LP

## Abstract

We present a simple mathematical model of fluid flow in a transverse cross section of a scraped-surface heat exchanger (SSHE). Specifically we use the lubrication approximation to analyse steady two-dimensional isothermal flow of a Newtonian fluid around a periodic array of pivoted scraper blades in a channel with one stationary and one moving wall. The analysis yields quantitative predictions that are directly relevant to the design and operation of SSHEs. In particular, the analysis reveals that there is a range of blade-pivot positions for which the desired contact between the blade tip and the scraped surface does not occur. The calculations also reveal details of the flow structure, including the possible presence of regions of reversed flow under the blades. In addition the forces on the blades and the torque on the rotor, as well as the fluxes of fluid above and below the blades, are all determined analytically. According to the simplest version of the model, when the desired blade contact is attained the associated forces and torque are singular. Two possible generalisations of the model (namely to a non-Newtonian power-law fluid and to include slip at the moving wall) are shown resolve these singularities.

## 1 Introduction

Scraped-surface heat exchangers (SSHEs), used widely in the food industry, comprise essentially a cylindrical steel annulus along which foodstuff is driven, and a ‘bank’ of blades rotating with the inner wall (the ‘rotor’) to scrape the foodstuff away from the heated or cooled outer wall (the ‘stator’), preventing fouling, and maintaining mixing and heat transfer (see figure 1). The processes that take place inside SSHEs are complex (see, for example, Härröd, 1986); features of the behaviour have been analysed recently by, for example, Stranzinger et al. (2001), Fitt

---

<sup>1</sup>Presenting author; email : [s.k.wilson@strath.ac.uk](mailto:s.k.wilson@strath.ac.uk)

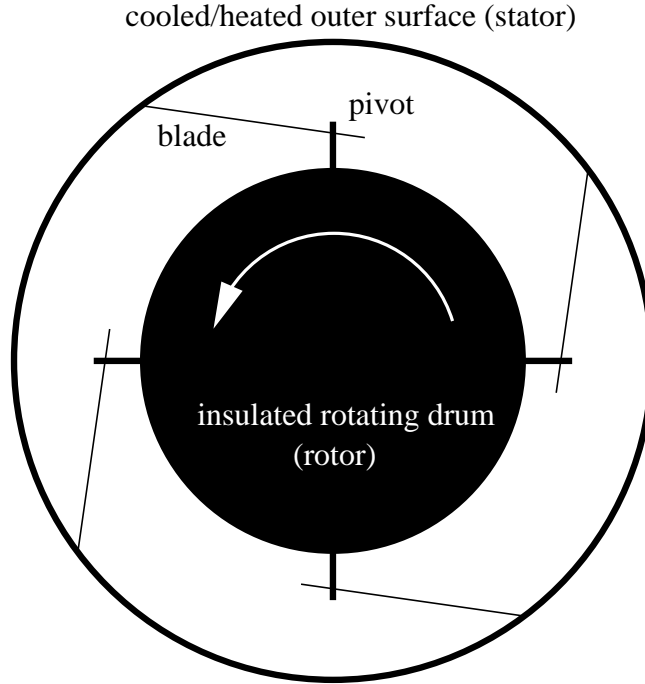


Figure 1: Sketch of a cross section of a SSHE.

& Please (2001) and Sun et al. (2004). In this paper we consider one aspect of the fluid flow in a SSHE, namely flow in the (annular) transverse cross section. In practice the gaps between the blades and the walls in a SSHE are fairly long and narrow, and so the ‘lubrication approximation’ may be used to analyse the flow. Thus we consider steady two-dimensional flow of an incompressible Newtonian fluid of viscosity  $\mu$  in a long parallel-sided channel of width  $H$  in which there is a periodic array of inclined smoothly pivoted thin plane blades, the flow being driven by the motion of one wall of the channel parallel to itself with speed  $U$  ( $> 0$ ), the other wall being fixed (see figure 2). In this preliminary study we are concerned only with the fluid flow in the channel, not the heat transfer, and so we consider only isothermal flow.

## 2 Blades not in contact with the channel walls

The blades are considered to be in equilibrium, subject to forces due to the fluid, the pivot, and (in general) the walls of the channel. First we consider the case of blades whose ends are *not* in contact with the channel walls.

We introduce Cartesian axes  $Oxyz$  with the wall  $y = 0$  moving with velocity  $U\mathbf{i}$ , and the wall  $y = H$  fixed. Suppose a blade occupies  $0 \leq x \leq L$ , with its pivot fixed at  $(x_p, h_p)$ , where  $0 \leq x_p \leq L$  and  $0 < h_p < H$ , and suppose that the portion  $L \leq x \leq L + \ell$  of the channel is ‘full

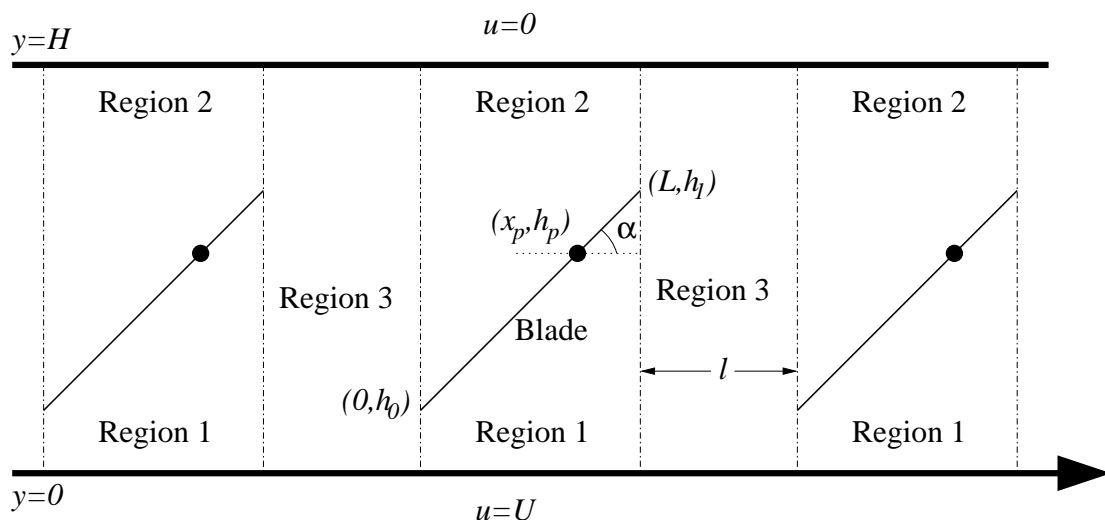


Figure 2: Geometry of the channel-flow problem. The blade pivots are shown as dots.

width'. This configuration is repeated periodically<sup>2</sup> with period  $L + \ell$ , so we need consider the flow only in the interval  $0 \leq x \leq L + \ell$ . The limit  $\ell \rightarrow \infty$  corresponds to the case of a single blade in a channel (and the limit  $H \rightarrow \infty$  of this case corresponds to the 'rocker bearing' in classical lubrication theory, studied extensively by, for example, Raimondi & Boyd, 1955a,b).

With  $\alpha$  denoting the (small) angle of inclination of the blade to the  $x$  axis, the blade is given by  $y = h(x)$ , where

$$h(x) = h_p + \alpha(x - x_p). \quad (1)$$

Also we let  $h_0 = h(0)$  and  $h_1 = h(L)$  ( $0 < h_0, h_1 < H$ ), so that

$$h_0 = h_p - \alpha x_p, \quad h_1 = h_p + \alpha(L - x_p), \quad \alpha = \frac{h_1 - h_0}{L}. \quad (2)$$

We denote the velocities, pressures, volume fluxes (per unit width) and stream functions by  $u_k \mathbf{i} + v_k \mathbf{j}$ ,  $p_k$ ,  $Q_k$  and  $\psi_k$ , where  $k = 1$  denotes values in  $0 \leq x \leq L$ ,  $0 \leq y \leq h$  (that is, the region 'below' the blade, termed 'region 1'),  $k = 2$  denotes values in  $0 \leq x \leq L$ ,  $h \leq y \leq H$  (that is, the region 'above' the blade, termed 'region 2'), and  $k = 3$  denotes values in  $L \leq x \leq L + \ell$ ,  $0 \leq y \leq H$  (termed 'region 3'). The lubrication approximation gives

$$\mu \frac{\partial^2 u_k}{\partial y^2} = \frac{\partial p_k}{\partial x}, \quad \frac{\partial p_k}{\partial y} = 0, \quad \frac{\partial u_k}{\partial x} + \frac{\partial v_k}{\partial y} = 0 \quad (3)$$

<sup>2</sup>In terms of the SSHE, the width  $H$ , speed  $U$  and period  $L + \ell$  here are defined by  $H = R_2 - R_1$ ,  $U = R_1 \omega$  and  $L + \ell = 2\pi R_1 / N$ , where  $R_1$  and  $R_2$  are the radii of the rotor and stator,  $N$  is the number of blades in a cross section of the SSHE, and  $\omega$  is the angular speed of the rotor.

for  $k = 1, 2, 3$ , to be solved subject to the no-slip condition on  $y = 0$ ,  $y = h$  and  $y = H$ . It is thus found that

$$u_1 = \frac{[6Q_1y + Uh(h - 3y)](h - y)}{h^3}, \quad (4)$$

$$u_2 = \frac{6Q_2(H - y)(y - h)}{(H - h)^3}, \quad (5)$$

$$u_3 = \frac{[6Q_3y + UH(H - 3y)](H - y)}{H^3}, \quad (6)$$

and

$$p_{1x} = \frac{6\mu U}{h^2} - \frac{12\mu Q_1}{h^3}, \quad p_{2x} = -\frac{12\mu Q_2}{(H - h)^3}, \quad p_{3x} = \frac{6\mu U}{H^2} - \frac{12\mu Q_3}{H^3}, \quad (7)$$

where the fluxes  $Q_k$  are constants (unknown as yet) satisfying the global mass-conservation condition

$$Q_1 + Q_2 = Q_3. \quad (8)$$

The pressure in each region is independent of  $y$ . Assuming that pressure is continuous at the ends of the blade, so that

$$p_1(L) = p_2(L) = p_3(L) \quad (= p_L, \text{ say}) \quad (9)$$

and

$$p_1(0) = p_2(0) = p_3(L + \ell) \quad (= p_0, \text{ say}), \quad (10)$$

we have from (7)

$$p_1 = \frac{6\mu U}{\alpha} \left( \frac{1}{h_1} - \frac{1}{h} \right) - \frac{6\mu Q_1}{\alpha} \left( \frac{1}{h_1^2} - \frac{1}{h^2} \right) + p_L, \quad (11)$$

$$p_2 = \frac{6\mu Q_2}{\alpha} \left[ \frac{1}{(H - h_1)^2} - \frac{1}{(H - h)^2} \right] + p_L, \quad (12)$$

$$p_3 = \frac{6\mu(UH - 2Q_3)}{H^3} (x - L) + p_L. \quad (13)$$

Setting  $x = 0$  in (11)–(12) and  $x = L + \ell$  in (13) we obtain three representations of  $p_0 - p_L$ , from which we deduce

$$U \left( \frac{1}{h_1} - \frac{1}{h_0} \right) - Q_1 \left( \frac{1}{h_1^2} - \frac{1}{h_0^2} \right) = Q_2 \left[ \frac{1}{(H - h_1)^2} - \frac{1}{(H - h_0)^2} \right] = \frac{\alpha(UH - 2Q_3)\ell}{H^3}. \quad (14)$$

The moment of the forces on the blade about the pivot due to the pressure is of the form  $\mathbf{M} = M\mathbf{k}$ , where

$$M = \int_0^L (x - x_p)(p_1 - p_2) dx. \quad (15)$$

Elimination of  $Q_1$ ,  $Q_2$  and  $Q_3$  between (8), (14) and the equilibrium condition  $M = 0$  leads to a lengthy algebraic transcendental equation of the form

$$F(\alpha, L, \ell, H, x_p, h_p) = 0 \quad (16)$$

(which is omitted for the sake of brevity). This equation is the key result determining  $\alpha$  when  $L$ ,  $\ell$ ,  $H$ ,  $x_p$  and  $h_p$  are prescribed; then with  $\alpha$  known, the complete solution ( $h_0$ ,  $h_1$ ,  $Q_k$ ,  $u_k$ ,  $p_k$  and  $\psi_k$  for  $k = 1, 2, 3$ ) is determined. Note that the solution  $\alpha$  of (16) is independent of  $\mu$  and  $U$ ; indeed  $\alpha$  is independent even of the sign of  $U$ .

Armed with the solution given above we can now describe all the qualitative features of the flow. We note that  $p_{3x}$  is a constant, but that  $p_{1x}$  and  $p_{2x}$  vary with  $x$ , in general. Also it may be shown from (8) and (14) that  $Q_k \geq 0$  and  $p_0 > p_L$ , and hence that  $p_{2x} \leq 0$  and  $p_{3x} > 0$  (though  $p_{1x}$ , on the other hand, may change sign). Moreover  $u_2$  (which is symmetric about  $y = \frac{1}{2}(h + H)$ ) satisfies  $u_2 \geq 0$  for all  $x$ , but the signs of  $u_1$  and  $u_3$  may change, that is, there may be backflow in regions 1 and 3. Specifically,  $u_1 = 0$  not only on the blade  $y = h$  but also on the curve  $y = y_{01}(x)$ , where

$$y_{01} = \frac{Uh^2}{3(Uh - 2Q_1)}, \quad (17)$$

in the region where  $h \geq 3Q_1/U$ ; such a region exists if  $h_0$ ,  $h_1$ ,  $Q_1$  and  $\alpha$  satisfy  $Uh_0 > 3Q_1$  (if  $\alpha < 0$ ) or  $Uh_1 > 3Q_1$  (if  $\alpha > 0$ ). In that case the curve (17) meets the blade  $y = h$  at the point where  $h = 3Q_1/U$ , which is a separation point; the separating streamline  $y = y_s(x)$  is given by

$$y_s = \frac{Q_1 h}{Uh - 2Q_1} \quad (< y_{01}). \quad (18)$$

Furthermore, (6) shows that the position  $y = y_{03}$  where  $u_3 = 0$  is given by

$$y_{03} = \frac{UH^2}{3(UH - 2Q_3)}, \quad (19)$$

so that  $0 < y_{03} < H$  (and there is backflow near the upper wall  $y = H$ ) if  $Q_3 < \frac{1}{3}UH$ .

The drag  $F_x$  and lift  $F_y$  on the blade are given by

$$F_x = \frac{2\mu}{\alpha} \left[ 3(h_1 - h_0) \left( \frac{Q_1}{h_1^2} + \frac{Q_2}{(H - h_1)^2} - \frac{U}{h_1} \right) + 2U \log \frac{h_1}{h_0} \right] \quad (20)$$

and

$$F_y = \frac{6\mu}{\alpha^2} \left[ (h_1 - h_0) \left( \frac{Q_1(h_1 - h_0)}{h_0 h_1^2} - \frac{Q_2(h_1 - h_0)}{(H - h_0)(H - h_1)^2} + \frac{U}{h_1} \right) - U \log \frac{h_1}{h_0} \right], \quad (21)$$

and the drag  $F_0$  on the portion  $0 \leq x \leq L + \ell$  of the wall  $y = 0$  is

$$F_0 = \frac{2\mu}{\alpha} \left[ \frac{3Q_1(h_1 - h_0)}{h_0 h_1} - 2U \log \frac{h_1}{h_0} \right] + \frac{2\mu}{H^2} (3Q_3 - 2UH)\ell. \quad (22)$$

An estimate of the torque (per unit width) required to turn the rotor of the SSHE is provided by  $-F_0 R_1 N$ , where  $R_1$  is the radius of the rotor and  $N = 2\pi R_1 / (L + \ell)$  is the number of blades.

To present results we take  $L$ ,  $h_p$ ,  $U$  and  $\mu UL/h_p^2$  as scales for length in the  $x$  direction, length in the  $y$  direction, velocity and pressure, respectively. Then equation (2) becomes

$$h_0 = 1 - \alpha x_p, \quad h_1 = 1 + \alpha(1 - x_p), \quad \alpha = h_1 - h_0, \quad (23)$$

and we have  $0 \leq x_p \leq 1$ ,  $0 < h_0, h_1 < H$  and  $H > 1$ . The geometrical restrictions  $h_0 > 0$ ,  $h_0 < H$ ,  $h_1 > 0$  and  $h_1 < H$  mean respectively that  $\alpha < \alpha_1(x_p, H)$ ,  $\alpha > \alpha_2(x_p, H)$ ,  $\alpha > \alpha_3(x_p, H)$  and  $\alpha < \alpha_4(x_p, H)$ , where

$$\alpha_1 = \frac{1}{x_p}, \quad \alpha_2 = -\frac{H-1}{x_p}, \quad \alpha_3 = -\frac{1}{1-x_p}, \quad \alpha_4 = \frac{H-1}{1-x_p}. \quad (24)$$

The form of the region in the  $(x_p, \alpha)$ -plane bounded by the curves (24) is sketched in figure 3; physically sensible solutions  $\alpha$  of (16) must lie in this ‘allowed’ region.

Figure 4 shows solutions  $\alpha$  of (16) as functions of  $x_p$  for several values of  $\ell$  in the case  $H = \frac{3}{2}$ ; the ‘bounding’ curves (24) (which depend on  $H$  but not  $\ell$ ) are also shown. The solution curves in figure 4 connect the bounding curves  $\alpha = \alpha_2$  ( $h_0 = H$ ) and  $\alpha = \alpha_4$  ( $h_1 = H$ ), but they do not in general intersect the bounding curves  $\alpha = \alpha_1$  ( $h_0 = 0$ ) and  $\alpha = \alpha_3$  ( $h_1 = 0$ ). It is found that the solution  $\alpha$  of (16) exists only for  $x_p$  lying in some interval  $x_{p,\min} \leq x_p \leq x_{p,\max}$ , where  $x_{p,\min}$  and  $x_{p,\max}$  depend on  $H$  and  $\ell$ .

For each  $H$  all the solution curves lie between those for  $\ell = 0$  and  $\ell = \infty$ . When  $\ell = 0$  the solution  $\alpha$  is determined uniquely by  $x_p$  for any  $H$ . On the other hand, for larger  $\ell$  (and, in particular, when  $\ell = \infty$ ) there can be up to three solutions  $\alpha$  for a given  $x_p$ , that is, there can be up to three equilibrium blade positions, each giving rise to a different flow pattern.

Figure 5 shows  $x_{p,\min}$  and  $x_{p,\max}$  plotted as functions of  $H$  for various values of  $\ell$ . The values of  $x_{p,\min}$  and  $x_{p,\max}$  are determined either by the positions  $x_p$  where  $d\alpha/dx_p = \infty$  (shown as heavy curves in figure 5), or by the intersections of the solution curve with the bounding curves  $\alpha = \alpha_2$  and  $\alpha = \alpha_4$  (shown as light curves in figure 5).

Figure 6 shows the force  $F_0$  given by (22) plotted as a function of  $x_p$  for  $H = \frac{3}{2}$  and various values of  $\ell$ . Cases in which  $F_0$  is multivalued as a function of  $x_p$  correspond to cases in which the  $(x_p, \alpha)$ -relation is multivalued. The curves for  $F_0$  are symmetric about a maximum at  $x_p = \frac{1}{2}$ , and the larger the value of  $\ell$ , the larger  $|F_0|$  is, in general.

Figure 7 shows the streamline pattern and some velocity profiles in regions 1 and 2, in a case with backflow in region 1, and with a rather weak flow in region 2 (so that  $Q_2$  is small).

### 3 Contact between the blade and a channel wall

As figure 4 shows, equation (16) (which determines the possible equilibrium positions of a blade that is *not* in contact with a wall of the channel) has solutions  $\alpha$  only when  $x_p$  is sufficiently close to  $\frac{1}{2}$ . In practice, however, the pivot position of a typical SSHE blade is near the right-hand end of the blade (so that  $x_p \simeq 1$ ), in which case equation (16) has no solution. We conclude that one of the ends of the blade must make contact with a channel wall. This means that the analysis leading to (16) must be modified to allow for blade contact.

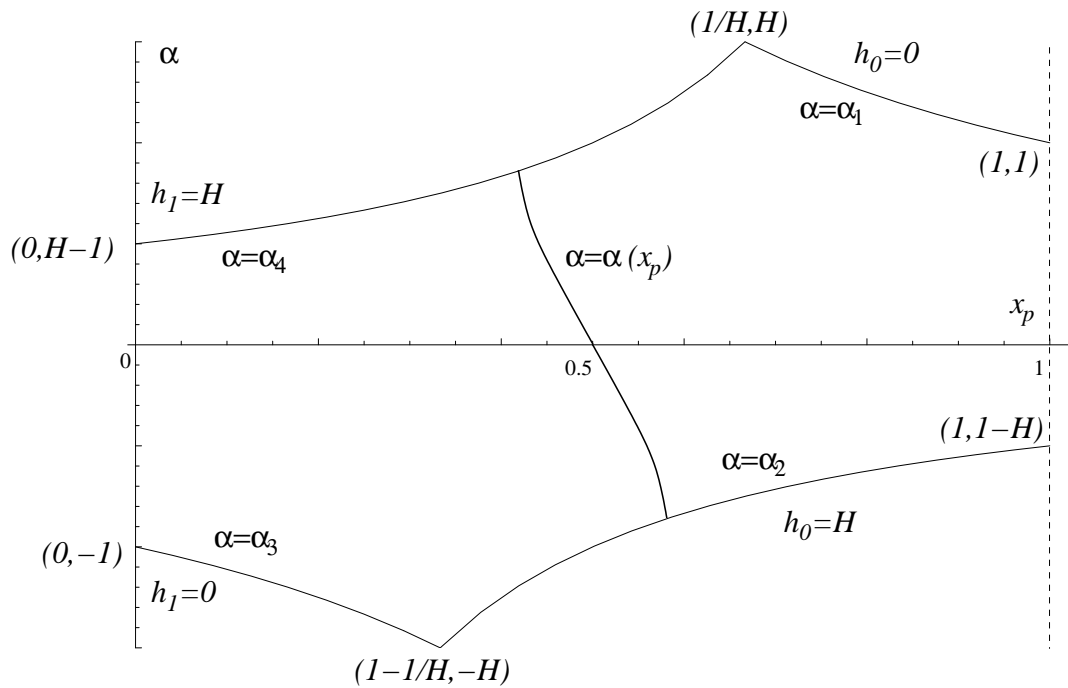


Figure 3: Sketch of the region in the  $(x_p, \alpha)$ -plane determined by (24) in which solutions  $\alpha(x_p)$  of equation (16) may lie.

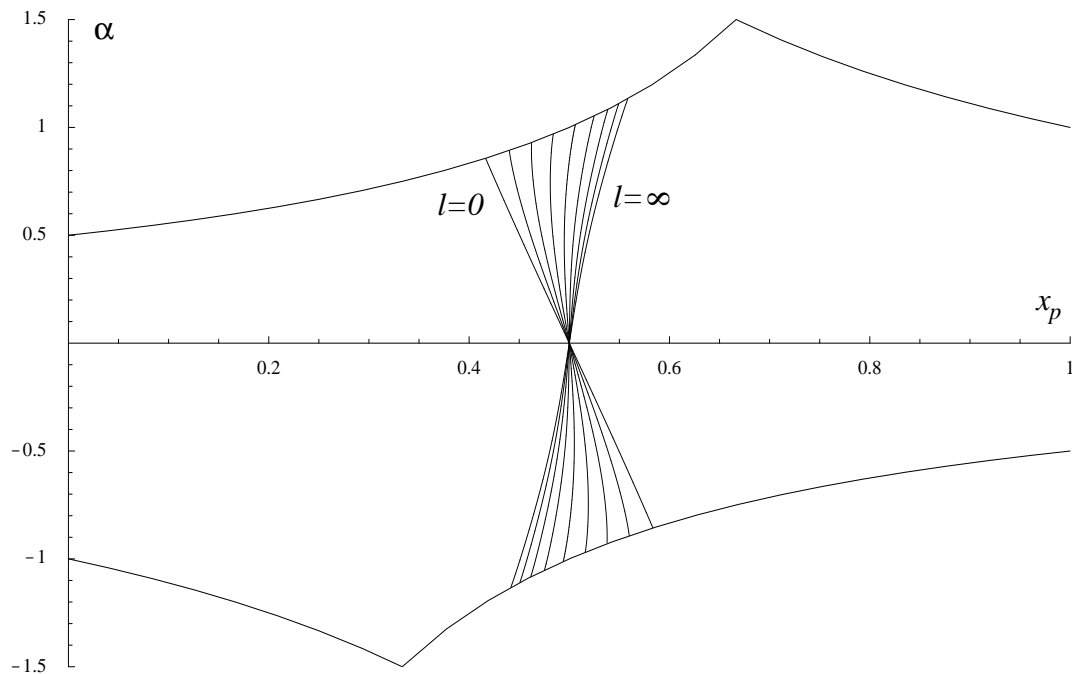


Figure 4: Plot of the solution  $\alpha(x_p)$  of equation (16) in the case  $H = \frac{3}{2}$ , for  $\ell = 0, \frac{1}{10}, \frac{1}{4}, \frac{1}{2}, 1, 2, 4, 10$  and  $\infty$ .

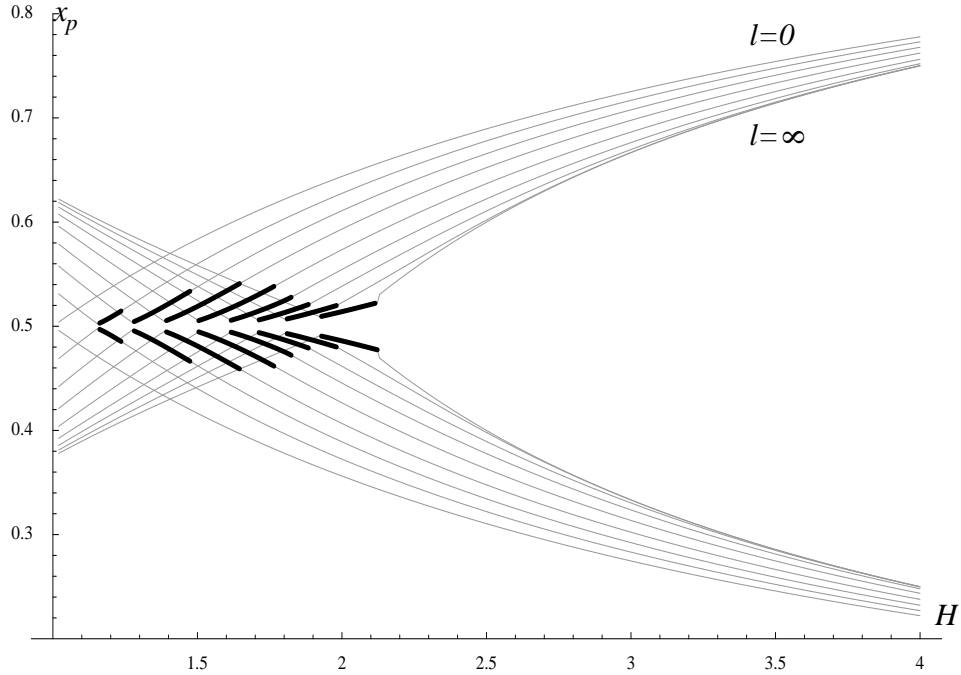


Figure 5: Plots of  $x_{p,\min}$  and  $x_{p,\max}$  as functions of  $H$  for  $\ell = 0, \frac{1}{10}, \frac{1}{4}, \frac{1}{2}, 1, 2, 4, 10$  and  $\infty$ . The light curves correspond to cases where one end of the blade is in contact with the wall  $y = H$  of the channel, so that  $\alpha = \alpha_2(x_p)$  or  $\alpha = \alpha_4(x_p)$ ; the heavy curves correspond to cases where the minimum and maximum values of  $x_p$  occur with the blade away from the channel walls.

### 3.1 A Newtonian fluid with no slip at the moving wall

Suppose that the blade touches the moving wall  $y = 0$  at the left-hand end<sup>3</sup> (that is, at  $x = 0$ , so that  $h_0 = 0$ , and as a consequence  $Q_1 = 0$  and  $Q_2 = Q_3$ ). We again take the blade to be given by  $y = h(x)$ , but now with

$$h(x) = \alpha x \quad (\alpha > 0). \quad (25)$$

All the results (3)–(14) are again found to hold (with  $h_0 = 0$ ,  $Q_1 = 0$ , and  $h_1 = h(L) = \alpha L < H$ ), except that the first equation in (14) must be dropped, and (10) must be replaced by

$$p_2(0) = p_3(L + \ell) \quad (= p_0, \text{ say}); \quad (26)$$

also the moment condition  $M = 0$  must be dropped.

It is found that

$$Q_2 = Q_3 = \frac{\alpha \ell U H (H - h_1)^2}{(2\alpha \ell - H)(H - h_1)^2 + H^3} \quad (27)$$

<sup>3</sup>The blade could also contact the walls at  $x = 0, y = H$ , at  $x = L, y = 0$ , or at  $x = L, y = H$ , but these cases are of less relevance to a real SSHE. The solution for a case in which the blade *just* touches the stationary wall  $y = H$  may be obtained simply by taking the appropriate (regular) limit of the results in Section 2.

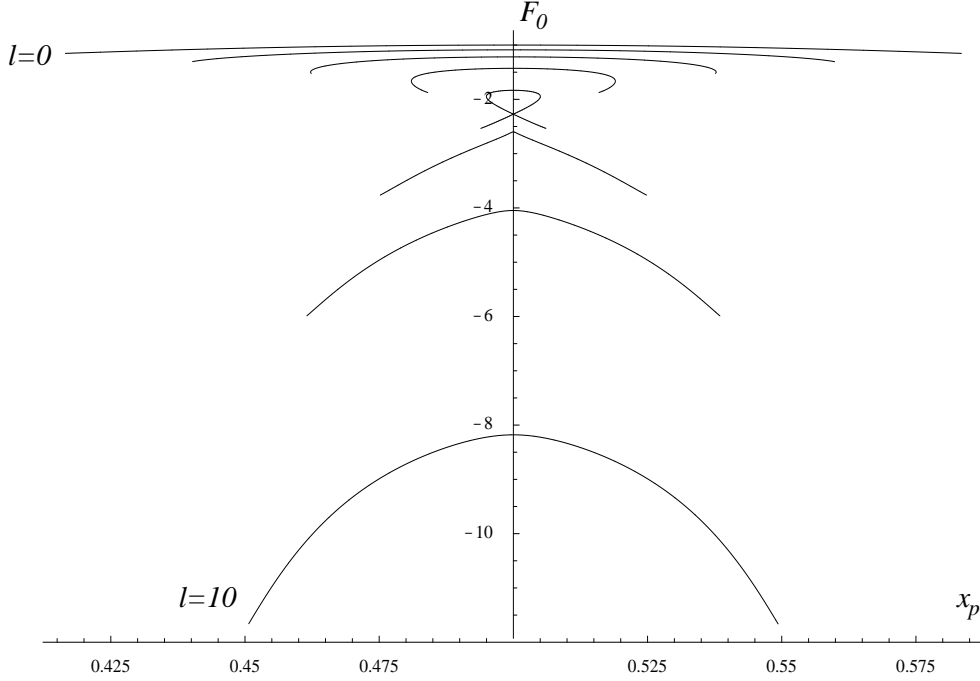


Figure 6: Plot of the force  $F_0$  on the moving wall  $y = 0$ , given by (22), as a function of  $x_p$  in the case  $H = \frac{3}{2}$ , for  $\ell = 0, \frac{1}{10}, \frac{1}{4}, \frac{1}{2}, 1, 2, 4$  and  $10$ .

and

$$p_0 - p_L = \frac{6\mu\ell U(2H - h_1)h_1}{H[(2\alpha\ell - H)(H - h_1)^2 + H^3]}. \quad (28)$$

We note from (27) that  $Q_2 > 0$ , so that  $p_{2x} < 0$ , and that  $UH - 2Q_3 > 0$ , so that  $p_{3x} > 0$ . Equation (4) shows that there is always backflow in the region  $0 \leq y \leq h$  under the blade, with  $u_{1y} = 0$  on  $y = y_{m1} = 2h/3$ , and  $u_1 = 0$  on  $y = y_{01} = h/3$ . Also  $y_{03}$  in (19) is given by

$$y_{03} = \frac{H}{3} + \frac{2\alpha\ell(H - h_1)^2}{3h_1(2H - h_1)} > \frac{H}{3} \quad (29)$$

(so that  $y_{03} < H$  only for sufficiently small  $\ell/L$ ).

However, this solution has a major shortcoming: equation (11) shows that in the limit  $x \rightarrow 0$

$$p_1 \sim -\frac{6\mu U}{\alpha^2 x} \rightarrow -\infty, \quad (30)$$

and the forces  $F_x$ ,  $F_y$  and  $F_0$  are infinite, and there is an infinite moment  $M$  on the blade tending to keep it in contact with the wall. In reality the stresses near the contact point  $x = 0$ ,  $y = 0$  may become large, but will, of course, remain finite; the singularities predicted above are a consequence of the simplifying assumptions concerning the two-dimensional nature of the problem, and the interaction between the fluid, the blade and the moving wall. Various alternative modelling assumptions may be invoked to alleviate these singularities; in particular,

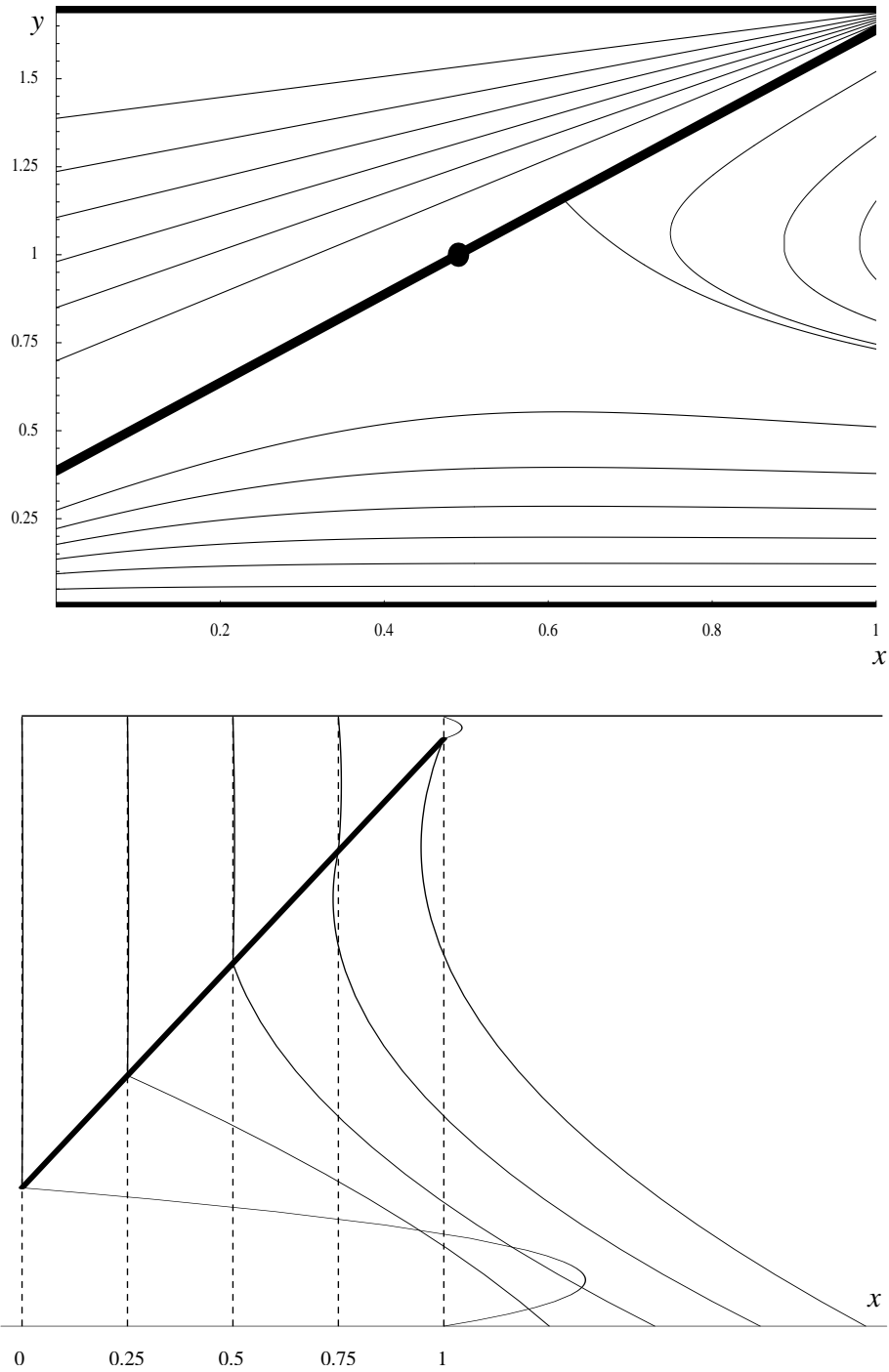


Figure 7: Plots of the streamline pattern and some velocity profiles in regions 1 and 2 in the case  $H = 1.7$ ,  $\ell = 2$ ,  $x_p = 0.49$ ,  $\alpha = 1.25322$ . (In this case the flow in region 2 is rather weak, so that  $Q_2$  is small.)

allowing non-Newtonian fluid behaviour or slip at the moving wall  $y = 0$  can achieve this, as we now describe.<sup>4</sup>

### 3.2 A power-law fluid with no slip at the moving wall

Consider an incompressible power-law fluid, with constitutive equation

$$\boldsymbol{\sigma} = 2\mu(q)\mathbf{e}, \quad \mu(q) = \mu_0[2 \operatorname{tr}(\mathbf{e}^2)]^{(n-1)/2}, \quad (31)$$

where  $\boldsymbol{\sigma}$  is the partial-stress tensor,  $\mathbf{e}$  is the rate-of-strain tensor, and  $\mu_0$  and  $n$  are constants (with  $n < 1$  for a shear-thinning fluid). For such a fluid the lubrication approximation gives (see, for example, Johnson & Mangkoesoebroto 1993; Ross et al. 1999)

$$\mu_0 \frac{\partial}{\partial y} \left( q_k^{n-1} \frac{\partial u_k}{\partial y} \right) = \frac{\partial p_k}{\partial x}, \quad \frac{\partial p_k}{\partial y} = 0, \quad \frac{\partial u_k}{\partial x} + \frac{\partial v_k}{\partial y} = 0, \quad q_k = \left| \frac{\partial u_k}{\partial y} \right| \quad (32)$$

for  $k = 1, 2, 3$ , to be solved subject to (9), (26) and no-slip conditions. For the sake of brevity we omit the full solution, and report only the form of the pressure  $p_1$ , namely

$$p_1 = - \left( \frac{(n+1+nb)U}{n} \right)^n \frac{\mu_0}{\alpha n b^{n+1}} \left( \frac{1}{h^n} - \frac{1}{h_1^n} \right) + p_L, \quad (33)$$

where  $b$  ( $\frac{1}{2} < b < 1$ ) is a constant, determined as a solution of the equation

$$(n+1+nb)(1-b)^{\frac{n+1}{n}} = n b^{\frac{2n+1}{n}}. \quad (34)$$

From (33) we have  $p_1 = O(x^{-n})$  as  $x \rightarrow 0$ , and so  $p_1$  is again singular, but now is integrable for  $n < 1$ , that is, the singularities in the forces and moment on the blade are resolved. Essentially the large shear rates near the contact point lead to a low viscosity there, and hence to stresses that, though singular, are integrable, giving finite forces.

Again there is always backflow in the region  $0 \leq y \leq h$  under the blade, with  $u_1 < 0$  for  $y > y_{01}$ , and  $u_1 > 0$  for  $y < y_{01}$ , where  $y = y_{01}$  satisfies

$$y_{m1} = \frac{1}{2}(h + y_{01}), \quad (35)$$

with the straight line  $y = y_{m1} = b\alpha x$  defining the position where  $u_{1y} = 0$ . Moreover, it may be shown that it is possible for  $u_3$  to be negative near  $y = H$ , that is, there can be backflow near  $y = H$  in region 3; in particular, this occurs when  $\ell/L$  is sufficiently small.

---

<sup>4</sup>Weidner & Schwartz (1994) showed that non-Newtonian (power-law) behaviour can alleviate the stress singularity at a three-phase contact line moving over a solid substrate; it is well known that slip at the substrate can have a similar effect. Silliman & Scriven (1978) showed that slip can alleviate the stress singularity occurring in viscous flow at a channel exit.

### 3.3 A Newtonian fluid with slip at the moving wall

We now consider the case of a Newtonian fluid that may slip along the moving wall  $y = 0$ , with relative velocity proportional to the local shear rate (see, for example, Greenspan 1978; Hocking 1981). The lubrication equations (3) must now be solved subject to (9), (26) and, in place of the no-slip condition,

$$u_1 - U = \beta u_{1y} \text{ on } y = 0, \quad u_1 = 0 \text{ on } y = h, \quad u_2 = 0 \text{ on } y = h, \quad u_2 = 0 \text{ on } y = H \quad (36)$$

in  $0 \leq x \leq L$ , and

$$u_3 - U = \beta u_{3y} \text{ on } y = 0, \quad u_3 = 0 \text{ on } y = H \quad (37)$$

in  $L \leq x \leq L + \ell$ , where  $\beta$  ( $\geq 0$ ) is a (small) slip length, which we take to be a constant.

These equations are solved in an analogous way to those in Section 2. In particular, it is found that

$$p_1 = \frac{3\mu U}{2\alpha\beta} \log \frac{h(h_1 + 4\beta)}{h_1(h + 4\beta)} + p_L. \quad (38)$$

Again there is always backflow under the blade, with  $u_{1y} = 0$  on  $y = y_{m1} = 2h/3$ , and  $u_1 = 0$  on  $y = y_{01} = h/3$ , exactly as in the no-slip case. Also  $p_{2x} < 0$  and  $p_{3x} > 0$ , as in the no-slip case. The position  $y = y_{03}$  where  $u_3 = 0$  is again given by (29), independent of  $\beta$ .

In the limit  $x \rightarrow 0$  we have

$$p_1 \sim \frac{3\mu U}{2\alpha\beta} \log \frac{\alpha(h_1 + 4\beta)x}{4\beta h_1}, \quad (39)$$

so again  $p_1 \rightarrow -\infty$  as  $x \rightarrow 0$ , but now  $p_1$  is integrable. In particular

$$F_x = \frac{2\mu}{\alpha} \left[ \frac{3Q_2 h_1}{(H - h_1)^2} + 2U \log \frac{h_1 + 4\beta}{4\beta} \right], \quad (40)$$

$$F_y = -\frac{6\mu}{\alpha^2} \left[ \frac{Q_2 h_1^2}{H(H - h_1)^2} + U \log \frac{h_1 + 4\beta}{4\beta} \right], \quad (41)$$

$$F_0 = -\frac{4\mu U}{\alpha} \log \frac{h_1 + 4\beta}{4\beta} + \frac{2\mu(3Q_3 - 2UH)\ell}{H(H + 4\beta)}, \quad (42)$$

and

$$M = \frac{3\mu}{\alpha^3} \left[ -Uh_1 + 2U(h_p + 2\beta) \log \frac{h_1 + 4\beta}{4\beta} + \frac{h_1 Q_2 (2H^2 - 3Hh_1 + 2h_1 h_p)}{H(H - h_1)^2} + 2Q_2 \log \frac{H - h_1}{H} \right], \quad (43)$$

all of which are finite for  $\beta > 0$ . In the singular limit  $\beta \rightarrow 0$  all these quantities are infinite, in agreement with the results from the no-slip case.

## 4 Conclusions

In this paper we presented a simple mathematical model of fluid flow in a transverse cross section of a scraped-surface heat exchanger (SSHE). Specifically we used the lubrication approximation to analyse steady two-dimensional isothermal flow of a Newtonian fluid around a periodic array of pivoted scraper blades in a channel with one stationary and one moving wall.

The present analysis yields quantitative predictions that are directly relevant to the design and operation of SSHEs. In particular, the analysis reveals that there is a range of blade-pivot positions  $x_{p,\min} \leq x_p \leq x_{p,\max}$  around  $x_p = \frac{1}{2}$  for which the desired contact between the blade tip and the scraped surface does not occur. Moreover, for such a value of  $x_p$  there can be as many as three different possible steady solutions each with different blade angles and flow patterns. The present calculations also reveal details of the flow structure, including the possible presence of regions of reversed flow under the blades. In addition the forces on the blades and the torque on the rotor, as well as the fluxes of fluid above and below the blades, were all determined analytically.

It was shown that locating the pivot sufficiently near the end  $x = L$  (as is typically done in actual SSHE designs) will ensure that the blade tip at  $x = 0$  will indeed make the desired contact with the scraped surface. However, the solution in this case predicts that the forces on the blades are singular and that an infinitely large torque is required to turn the rotor. These unrealistic predictions indicate that one or more factors neglected in the simple model become significant in this case. Two possible generalisations of the model (namely to a non-Newtonian power-law fluid and to include slip at the moving wall) were shown to resolve these singularities.

The preliminary model presented here adds to the quantitative understanding of some of the basic features of the fluid flow within a SSHE. We intend to extend our analysis to investigate other practically important features neglected in this simple model, including axial flow (that is, flow in the  $z$  direction), blade wear and, of course, non-isothermal effects.

## Acknowledgements

Thanks are due to Profs C. P. Please and A. D. Fitt, Faculty of Mathematical Studies, University of Southampton, Prof. D. L. Pyle and Dr K.-H. Sun, School of Food Biosciences, University of Reading, Dr J. Mathisson, Tetra Pak, and Dr H. Tewkesbury, Smith Institute, for many useful discussions. This work forms part of a larger research project supported by the EPSRC (Research Grant GR/R993032, Principal Investigator Prof. C. P. Please), and by Chemtech International Ltd and Tetra Pak, under the auspices of the Faraday Partnership for Industrial Mathematics, managed by the Smith Institute.

# Nomenclature

- $x, y, z$  ... Cartesian coordinates,  
 $\mu$  ... viscosity,  
 $U\mathbf{i}$  ... velocity of the wall  $y = 0$ ,  
 $u_k\mathbf{i} + v_k\mathbf{j}$  ... fluid velocity in region  $k$  ( $= 1, 2, 3$ ),  
 $p_k$  ... pressure in region  $k$ ,  
 $\psi_k$  ... stream function in region  $k$ ,  
 $Q_k$  ... volume flux (per unit width) in region  $k$ ,  
 $H, L, \ell$  ... channel width, blade length and inter-blade separation,  
 $R_1, R_2$  ... radii of the rotor and stator,  
 $\omega$  ... angular speed of the rotor,  
 $N$  ... number of blades in the SSHE,  
 $x_p, h_p$  ... coordinates of the blade pivot,  
 $\alpha$  ... inclination angle of the blade,  
 $h(x) = h_p + \alpha(x - x_p)$  ... shape of the blade,  
 $h_0, h_1$  ... heights of the ends of the blade at  $x = 0$  and  $x = L$ ,  
 $p_0, p_L$  ... pressures at  $x = 0$  and  $x = L$ ,  
 $\mathbf{M} = M\mathbf{k}$  ... moment of forces on the blade,  
 $F_x, F_y$  ... drag and lift (per unit width) on the blade,  
 $F_0$  ... drag (per unit width) on the wall  $y = 0$  ( $0 \leq x \leq L + \ell$ ),  
 $x_{p,\min} \leq x_p \leq x_{p,\max}$  ... pivot positions  $x_p$  for which blade contact does not occur,  
 $\alpha_1, \alpha_2, \alpha_3, \alpha_4$  ... bounding curves in the  $(x_p, \alpha)$ -plane,  
 $y = y_{01}(x), y = y_{03}(x)$  ... curves on which  $u_1 = 0$  and  $u_3 = 0$ ,  
 $y = y_{m1}(x), y = y_{m3}(x)$  ... curves on which  $u_{1y} = 0$  and  $u_{3y} = 0$ ,  
 $y = y_s(x)$  ... separating streamline in region 1,  
 $\boldsymbol{\sigma}, \mathbf{e}$  ... stress tensor and rate-of-strain tensor,  
 $\mu_0, n$  ... parameters of a power-law fluid,  
 $b$  ...  $n$ -dependent parameter defined by equation (34),  
 $\beta$  ... slip coefficient.

## References

- FITT, A. D. & PLEASE, C. P. 2001 Asymptotic analysis of the flow of shear-thinning food-stuffs in annular scraped heat exchangers. *J. Engng Maths* **39**, 345–366.
- GREENSPAN, H. P. 1978 On the motion of a small viscous droplet that wets a surface. *J. Fluid Mech.* **84**, 125–143.
- HÄRRÖD, M. 1986 Scraped surface heat exchangers: a literature survey of flow patterns, mixing effects, residence time distribution, heat transfer and power requirements. *J. Food Proc. Eng.* **9**, 1–62.
- HOCKING, L. M. 1981 Sliding and spreading of thin two-dimensional drops. *Q. J. Mech. Appl. Math.* **34**, 37–55.
- JOHNSON, M. W. & MANGKOESOE BROTO, S. 1993 Analysis of lubrication theory for the power law fluid. *Trans. ASME J. Tribol.* **115**, 71–77.
- RAIMONDI, A. A. & BOYD, J. 1955a Applying bearing theory to the analysis and design of pad-type bearings. *Trans. ASME* **77**, 287–309.
- RAIMONDI, A. A. & BOYD, J. 1955b The influence of surface profile on the load capacity of thrust bearings with centrally pivoted pads. *Trans. ASME* **77**, 321–330.
- ROSS, A. B., WILSON, S. K. & DUFFY, B. R. 1999 Blade coating of a power-law fluid. *Phys. Fluids* **11**, 958–970.
- SILLIMAN, W. J. & SCRIVEN, L. E. 1978 Slip of liquid inside a channel exit. *Phys. Fluids* **21**, 2115–2116.
- STRANZINGER, M., FEIGL, K. & WINDHAB, E. 2001 Non-Newtonian flow behaviour in narrow annular gap reactors. *Chem. Engng Sci.* **56**, 3347–3363.
- SUN, K.-H., PYLE, D. L., FITT, A. D., PLEASE, C. P., BAINES, M. J. & HALL-TAYLOR, N. 2004 Numerical study of 2D heat transfer in a scraped surface heat exchanger. *Computers & Fluids* **33**, 869–880.
- WEIDNER, D. E. & SCHWARTZ, L. W. 1994 Contact-line motion of shear-thinning liquids. *Phys. Fluids* **6**, 3535–3538.